**US Army Corps
of Engineers**
Waterways Experiment
Station

Approximation of Electromagnetic Profiles

by   Falih H. Ahmad

19960604 030

DTIC QUALITY INSPECTED 1

The contents of this report are not to be used for advertising,
publication, or promotional purposes. Citation of trade names
does not constitute an official endorsement or approval of the use
of such commercial products.

Approximation of Electromagnetic Profiles

by Falih H. Ahmad

U.S. Army Corps of Engineers
Waterways Experiment Station
3909 Halls Ferry Road
Vicksburg, MS   39180-6199

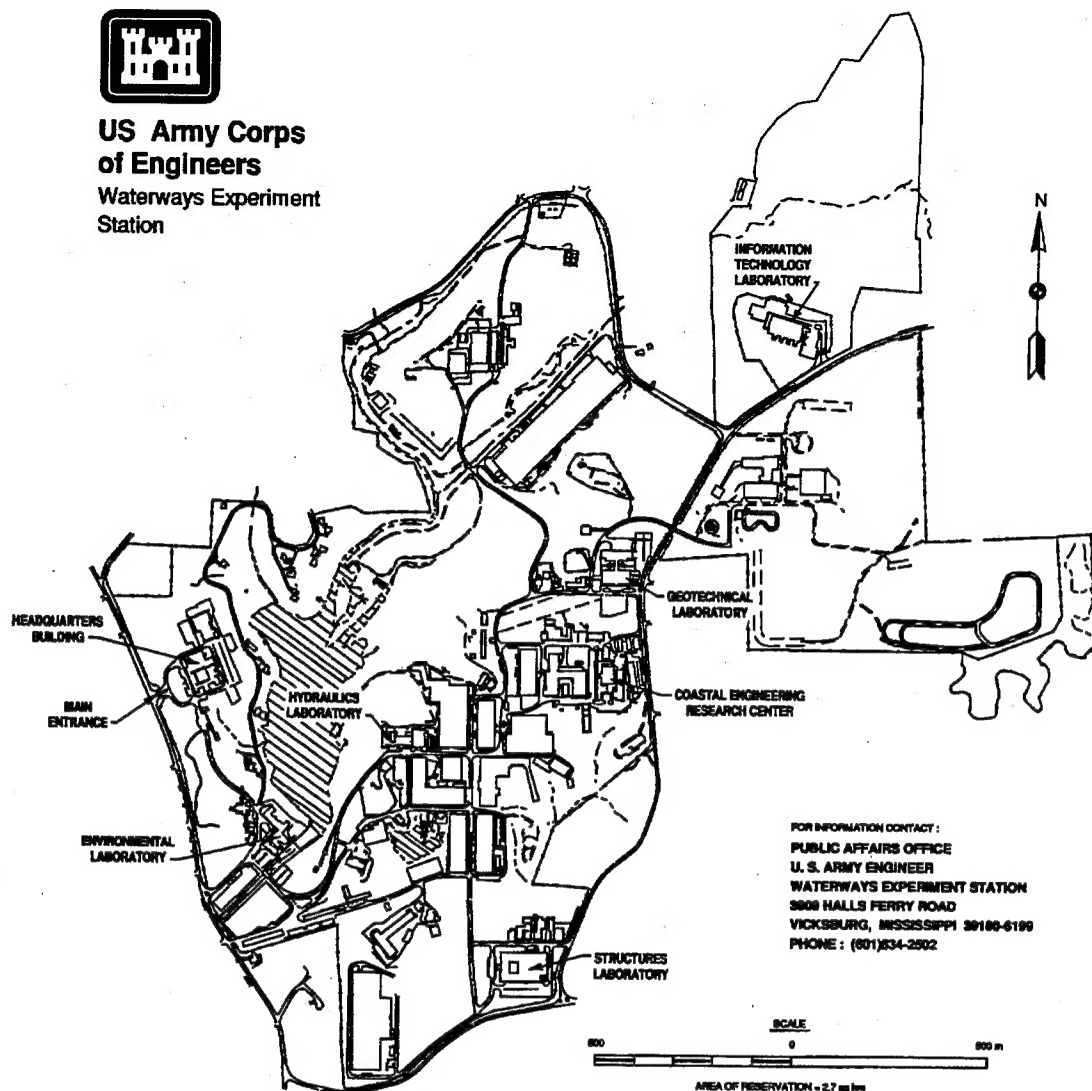Final report

Approved for public release; distribution is unlimited

US Army Corps of Engineers
Waterways Experiment Station

Contents

List of Tables

Preface

This study was conducted under the Discretionary Research Program sponsored by the U.S. Army Engineer Waterways Experiment Station (WES). The work was conducted during the period October 1993 to September 1995.

The research was conducted by Dr. Falih H. Ahmad, Instrumentation Systems Development Division, Information Technology Laboratory, WES, under the general supervision of Dr. N. Radhakrishnan, Director, Information Technology Laboratory; and Mr. George P. Bonner, Chief, Instrumentation Systems Development Division.

During the preparation of this report, Dr. Robert W. Whalin was Director of WES. Commander was COL Bruce K. Howard, EN.

This report should be cited as follows:

1　Introduction

Background

Much effort is spent in improving methods used to remotely characterize media or objects, which may be referred to as media identification. In general, media are identified using electromagnetic or acoustic energy. In the case of electromagnetic energy, radar is used to perform such tasks. In particular, a high-resolution radar is considered well suited to perform media identification. Electromagnetic and acoustic methods are being used at the U.S. Army Engineer Waterways Experiment Station in many research programs for automatic detection and identification of subsurface mines, moisture contents, and material characterization.

Target identification sequence is of three parts: detection, discrimination, and recognition. Feature extraction from the reflected electromagnetic energy is performed in the latter for three reasons: (a) to optimize recognition system performance, (b) to reduce the amount of information to be processed, and (c) to ensure robustness or invariance of the recognition system. For example, a set of features may actually be composed of the fast Fourier transform of the reflected energy; target's radar cross section (RCS); and the permittivity, velocity of propagation, permeability, susceptibility, and conductivity profiles of the medium in which the target exists. While the target's RCS is produced through the application of radar methods, application of inverse scattering theory is used to construct the mentioned profiles (Eaves and Reedy 1987). Let a medium or target be a scatterer. An incoming incident wave impinging upon the scatterer will produce a reflected wave and a transmitted wave. The direct scattering problem is to determine the reflected and transmitted waves if the incident wave and properties of the scatterer are known. In general, the inverse scattering problem is to determine the properties of the scatterer, given the incident, reflected, and transmitted waves. Inverse scattering problems have numerous practical applications in seismology, target identification, subsurface and ground-penetrating radar, geophysical sensing, medical imaging, and nondestructive testing. For example, in radar or sonar theory a known incident wave and observed reflected wave are used to detect the properties and presence of objects. This is an inversion process. Also, in the operations of nondestructive testing of media and remote sensing, it is desired to apply target or pattern recognition to identify objects, defects, or any other kind of

targets and discriminate between them and clutter. In the case where electromagnetic energy is utilized to serve this purpose, the electromagnetic profiles mentioned earlier in this section are considered important parts of the recognition process. They are used in the recognition process to characterize the different media. From the physical point of view it should be noted that different bodies, media, or materials possess different profiles of electromagnetic properties as seen from models of such properties. Take, for example, the simple model for the permittivity of a dispersive medium given in Jackson (1975). In this case the equation of motion for a charge is bounded by a harmonic force and acted on by an electric field and the effects of the magnetic force are neglected. As a result the permittivity is described as a function of the number of the molecules per unit volume, the number of the electrons per molecule, and a damping constant. Thus, the permittivity profile of every material is unique. Accordingly, a target recognition process that utilizes reflection, conductivity, permittivity, and permeability profiles of media is considered a dependable process. Improvement in the speed with which the results are generated through this process and their accuracy is logically vital for any military mission such as the automatic detection and identification of subsurface mines. Solutions of inverse problems are used for the generation of the electromagnetic profiles utilized in automatic recognition processes.

Inverse problems and their corresponding solutions have been formulated in many fashions. They are in the form of integro-differential, partial, or ordinary differential equations. Some of these problems are formulated in the time domain and others in the frequency domain. The electromagnetic profiles are taken to be functions of depth in the medium, time, or frequency. For example, various methods of reconstructing different profiles through inversion are presented in Wolfgang-Martin, Jordan, and Kay (1981); Kristensson and Krueger (1986); Ladouceur and Jordan (1985); Kreider (1989); Bleistein and Cohen (1977); Jordan and Kritikos (1973); Ge (1987); and Cui and Liang (1993, 1994b). Examples of the application of iterative numerical methods to the solution of inverse problems are presented in Devaney (1983); Tijhuis and Van Der Worm (1984); and Chew and Wang (1990). Consequently, methods of rating numerical methods used to solve a given inverse problem are accuracy of data they generate, efficiency of time required by the method, length of computational time, method implementation, and realization. Improvement of the inversion process may be carried out in the formula used. Take for example the approximate inversion formula derived in Ladouceur and Jordan (1985). This formula implicitly relates the permittivity profile of an unknown lossless medium with the Fourier transform of the reflection coefficient. However, this formula breaks down when the discontinuity at the interface between the dielectric medium and free space is large. It also breaks down in the deeper regions in the medium. A network method is formulated in Cui and Liang (1993) to invert the permittivity profile of a half-space inhomogeneous medium. This method is compared with that in Ladouceur and Jordan (1985) and it is shown that it can take into account possible discontinuities at the free space-dielectric medium interface. Moreover, as it is demonstrated in Cui and Liang (1993), the network method formulation can be used in shallow and deeper regions as well; thus some improvement in the inversion process has

2

been achieved. This leads to a better material characterization and target identification. Enhancement of inversion processes is also achieved through improvements of numerical methods utilized in such processes.

Examples of inverse problem formulation may include the availability of the reflection of a perpendicularly polarized, time-harmonic plane wave with a known wave number incident at a given angle on an inhomogeneous region with unknown permittivity. The permittivity of the medium is considered a function of the wave number used and depth in the medium. The inverse problem is to construct the permittivity profile relative to that of free space. This construction is accomplished through the use of the complex reflection coefficient. In this example the inverse scattering problem is formulated in the frequency domain and the medium is considered dispersive (Jordan and Kritikos 1973). In a second example a half-space inhomogeneous pure conducting medium is considered. A time-harmonic plane-polarized electromagnetic wave of a known wave number is incident from the free space region upon the medium at a known oblique angle. In this example the complex reflection coefficient is used to represent the scattering energy, and it is used to construct the conductivity profile of the medium (Ge 1987). A third example is formulated in the frequency domain where the considered electromagnetic energy is scattered from a one-dimensional inhomogeneous and lossless dielectric slab of a given thickness embedded in the vacuum. Using this scattered energy, an approximate permittivity profile of the slab is generated (Cui and Liang 1994b). Another inverse problem formulation includes scattering by a one-dimensional inhomogeneous lossy dielectric slab of known thickness embedded in the vacuum. The permittivity and the conductivity of the slab are unknown and assumed to be real. An electromagnetic pulse of finite duration is incident on the slab, and the electric field inside the slab is presented in the form of an integral equation (Cui and Liang 1993). Approximate permittivity and conductivity profiles are generated as a result of solving this inverse problem.

In practice, situations are rarely encountered in which a one-dimensional model for the inverse scattering problem can be used, whereas a two-dimensional model proves to be suitable for a large class of problems. A class of solutions targets the general nonlinear inverse problem. Thus far, no numerical solutions have been produced for these methods apparently due to their inherent instabilities. There have been hosts of other solutions, especially those reported in connection with elastic waves in seismic exploration, that use optimization and iterative techniques (Santosa et al. 1984). Although these are valid methods, their sensitivity to experimental and numerical noise results in inaccurate solutions and poor resolution. Also, a variety of frequency-domain solutions to the two-dimensional inverse scattering problem exist based on the assumption of weak scattering. The Born approximation is one such method which solves the linear inverse problem. These approaches are not valid for the more general cases in which strong diffraction and multiple scattering effects are present (Moghaddam 1991). Another class of solutions targets the general nonlinear inverse problem for Schrödinger-type equations (Newton 1981). This kind of approach has been treated in connection with evaluation

of an optical pulse in a graded-index, single-mode, nonlinear optical fiber. In this approach a differential equation of the nonlinear Schrödinger-type equation is obtained. The unknown in this equation is the envelope of a pulse propagating through the optical fiber. As a result of applying the inverse scattering method an equivalent system of Gel'fand-Lavitan-Marchenko coupled integral equations is formulated and an approximate to the unknown envelope is generated (Frangos and Frantzeskakis 1993).

Solution of the inverse problem is applied to reduce an earthquake hazard. It is used to better understand the earthquake processes and the properties of the rock in the focal region. In this case seismographs are used to detect and record ground motion caused by the passage of elastic waves from earthquakes. The challenge in this case is the determination of the earthquake source parameters and the seismic properties of the earth from a set of observations made near the earth's surface. In this application teleseismic observations or P-wave arrival times from local earthquakes are inverted for the purposes stated above (Santosa et al. 1984).

Purpose

This investigation is a research in which efforts are made to formulate an inversion scheme. The scheme should generate accurate electromagnetic profiles. Also, this scheme should perform accurately in shallow regions and deep regions as well. It should have a fast rate of convergence. In this report this scheme is formulated and used to generate permittivity and susceptibility profiles. The scheme is tested in shallow and deep regions. Also, effectiveness, accuracy, and rate of convergence of the formulated scheme are considered. In addition, the scheme's immunity to noise and its stability are explored. The formulation of the inversion scheme proposed in this report is applied to three selected cases to test its effectiveness. However, the scheme's parametric study, stability, immunity to noise, and its application to higher dimensions will be conducted in a subsequent investigation. Once the formulated scheme is tested and evaluated, it will be used as a part of a target identification and classification process. One objective in this process is to generate permittivity, velocity of propagation, permeability, and conductivity profiles effectively and accurately. A high-resolution radar is designed to generate the electromagnetic energy used in this process and to evaluate the formulated inversion scheme. This evaluation will be performed in the laboratory under controlled conditions and followed by an evaluation in the field. In this report, criteria and requirements of the high-resolution radar are addressed. The development of this radar will be completed in subsequent work.

Scope

Different formulations of the inverse problem are given and discussed in this report. The inversion scheme proposed in this report is applied to three

4

selected cases. Results from this application are compared with those generated through the application of previous approximation methods, analytical deductions, or exact expressions. In the inversion scheme proposed in this report a spectral collocation method found in Canuto et al. (1988) is utilized. Through this utilization N^{th} degree interpolating polynomials are constructed to approximate functions involved in the formulation. These polynomials are defined by using Legendre-Gauss-Lobatto points as the collocation points and Lagrange polynomials as the trial functions. Research materials related to the inverse problem are given in Chapter 2.

In radar applications, high-range resolution can be achieved by transmitting a low-peak-power, coded pulse of long duration and then compressing it on reception. A radar system that incorporates pulse compression processing provides improved detection performance, reduction in the mutual interference, and an increase in the system operational flexibility (Eaves and Reedy 1987). This information is used as a basis for the design and development of the high-resolution radar that will be used in the evaluation of the formulated inversion scheme. At the present time Barker codes are selected to form the coded transmitted pulses. A brief description and properties of these codes are given in this report. The inverse problem solution is given in Chapter 2. Research materials related to the high-resolution radar are given in Chapter 3. Conclusions, recommendations, and comments are given in Chapter 4.

2   Inverse Problem Solution

Formulations of the Inverse Problem

A general form of the solution of the inverse problem consists of determining the coefficients of a partial differential equation from the knowledge of the asymptotic behavior of the solution (Weston 1972). Maxwell's equation for the electromagnetic propagation in a direction along the z-axis normal to a slab of varying permittivity $\varepsilon(z)$[1] and conductivity $\sigma(z)$ is in the following form (Krueger 1978):

$$E_{zz}\ (z,t) - \varepsilon(z)\ \mu_0\ E_{tt}\ (z,t) - \sigma\ (z)\ \mu_0\ E_t\ (z,t) = 0 \tag{1}$$

where

$E(z,t) =$ electric intensity

$\mu_0 =$ permeability

$z =$ depth in the medium

$t =$ time

In Equation 1 the permeability μ_0 is constant, i.e., the medium is considered nonmagnetic. In this formulation the permittivity and conductivity of the medium are functions of depth only. The slab is bounded by free space where the permittivity is ε_0 and the conductivity is zero. Using the transformation

$$x(z) = \int_0^z \sqrt{\mu_0\ \varepsilon(s)}\ ds, \ H = x(L) \tag{2}$$

---

[1] For convenience, a list of symbols is found in the Notation (Appendix A).

where

s = dummy variable of integration

H = the value of the variable x when $z = L$

L = maximum value of the variable z

Equation 1 is transformed to

$$E_{xx}(x,t) - E_{tt}(x,t) + A(x)E_x(x,t) + B(x)E_t(x,t) = 0 \qquad (3)$$

where

$$A(x) = -\frac{d}{dz} \cdot \frac{1}{\sqrt{\mu_0\varepsilon(z)}} \ , \ B(x) = -\frac{\sigma(z)}{\varepsilon(z)}$$

At time $t = 0$ the electric field impinges upon the inhomogeneous medium, i.e., the slab. In the process, a left-moving reflected electromagnetic wave is produced. To model this physical action, the electromagnetic field $E(x,t)$ is split into $E^\pm(x,t)$ components by the decomposition

$$E^\pm(x,t) = \frac{1}{2} \ [E(x,t) \mp \int_0^t E_x(x,s) \ ds] \qquad (4)$$

In Equation 4 $E^-(x,t)$ and $E^+(x,t)$ are the left- and the right-moving electromagnetic waves, respectively. The relationship between $E^-(x,t)$ and $E^+(x,t)$ in the inhomogeneous medium is defined through

$$E^-(x,t) = \int_0^t r(x,s)E^+(x,t - s) \ ds \qquad (5)$$

In Equation 5 $r(x,t)$ is the impulse response of the inhomogeneous medium (Santosa et al. 1984). The impulse response satisfies the following equations

$$r_x(x,t) - 2r_t(x,t) = -B(x)r(x,t) - \frac{1}{2} \ [A(x) + B(x)]r * r(x,t) \qquad (6)$$

$$r(x,0) = -\frac{1}{4} \ [A(x) - B(x)] \qquad (7)$$

$$r(H,t) = 0 \tag{8}$$

where

$$r * r(x,t) = \int_0^t r(x,s)\, r(x,t - s)\, ds$$

In application the impulse response at $x = 0$, i.e., $r(0,t)$, is given. Consequently, the inverse problem could be stated as follows: given the function $r(0,t)$ what are the permittivity and conductivity profiles of the inhomogeneous medium? Equations 6-8 along with the given function $r(0,t)$ form a solution for the inverse problem. However, it should be noted that one of the functions $A(x)$ or $B(x)$ should be also known in order to generate the other. In the case when neither of the functions $A(x)$ nor $B(x)$ is known, one is forced to assume $A(x)$ or $B(x)$ and solve for the other. In application the function $r(0,t)$ is generated from a measurement procedure. Numerical techniques are applied to solved for the unknown profile. Effects of parametric changes, noise, rate of convergence, accuracy, length of computational time, methods of implementation, and realization are all merits on which the particular technique is evaluated. Obviously, the assumption of one of the profiles along with the complexity of the process of selecting one particular numerical technique is considered very important since the results from this stage are used in the target identification process.

In an alternative method the inverse problem is formulated in terms of the frequency domain reflection coefficient of the medium (Cui and Liang 1993). In this case a time-harmonic transverse electromagnetic (TEM) wave of wave number κ is normally incident on the interface of a half-space dielectric inhomogeneous medium. The depth in the medium is given the variable x. At the point x the frequency domain reflection coefficient of the medium is $\rho(\kappa,x)$ and at the point $x + dx$ it is $\rho(\kappa,x) + d\rho(\kappa,x)$. The medium is regarded as a transmission line network and the interface between the medium and free space is considered a junction in this network. The scattering matrix, S, of this transmission line junction is

$$S = \begin{bmatrix} d\Gamma & \sqrt{1 - (d\Gamma)^2} \\ \sqrt{1 - (d\Gamma)^2} & -d\Gamma \end{bmatrix} \tag{9}$$

where

8

$$dΓ = \frac{Z(x + dx) - Z(x)}{Z(x + dx) + Z(x)} \qquad (10)$$

$Z(x)$ and $Z(x+dx)$ are the wave impedances at the points x and $x+dx$ respectively. Considering the relationships

$$Z(x) = \frac{120\pi}{\sqrt{\varepsilon(x)}} \qquad (11)$$

$$\varepsilon(x + dx) = \varepsilon(x) + \frac{d\varepsilon(x)}{dx} \cdot dx \qquad (12)$$

one can write Equation 10 as

$$dΓ = \frac{\sqrt{\varepsilon(x)} - \sqrt{\varepsilon(x + dx)}}{\sqrt{\varepsilon(x)} + \sqrt{\varepsilon(x + dx)}} \approx$$

$$\frac{\sqrt{\varepsilon(x)} - \left[\sqrt{\varepsilon(x)} + \frac{1}{2} \cdot \frac{d\varepsilon(x)}{\sqrt{\varepsilon(x)}}\right]}{\sqrt{\varepsilon(x)} + \left[\sqrt{\varepsilon(x)} + \frac{1}{2} \cdot \frac{d\varepsilon(x)}{\sqrt{\varepsilon(x)}}\right]} \qquad (13)$$

$$= -\frac{d\varepsilon(x)}{4\varepsilon(x)}$$

Using microwave network theory, the frequency domain reflection coefficient of the medium, $\rho(\kappa,x)$, can be written as

$$\rho(\kappa,x) = \left\{ dΓ + \frac{[1 - (dΓ)^2][\rho(\kappa,x) + d\rho(\kappa,x)]}{1 + \rho(\kappa,x)\, dΓ + d\rho(\kappa,x)\, dΓ} \right\} \qquad (14)$$
$$\cdot\, e^{-j2\,\kappa\sqrt{\varepsilon(x)}\,dx}$$

Neglecting $(dΓ)^2$, $(dΓ)^4$ and $d\rho dΓ$ terms, Equation 14 reduces to

$$\rho(\kappa,x) = \left[dΓ + \frac{\rho(\kappa,x) + d\rho(\kappa,x)}{1 + \rho(\kappa,x)\, dΓ} \right] \cdot e^{-j2\,\kappa\sqrt{\varepsilon(x)}\,dx}$$

or

$$\rho(\kappa,x) \left[1 + \rho(\kappa,x) \, d\Gamma\right] = \left[d\Gamma + \rho(\kappa,x)\right.$$

$$\left.(d\Gamma)^2 + \rho(\kappa,x) + d\rho(\kappa,x)\right] e^{-j2\kappa\sqrt{\varepsilon(x)}dx}$$

Again neglecting $(d\Gamma)^2$ and using $e^x \approx 1+x$ yields

$$\rho\,(\kappa,x) + [\rho(\kappa,x)]^2 \, d\Gamma =$$

$$d\Gamma + \rho(\kappa,x) + d\rho(\kappa,x) - j2\kappa\sqrt{\varepsilon(x)} \; dx \; d\Gamma -$$

$$\rho(\kappa,x) \, j2\kappa\sqrt{\varepsilon(x)} \; dx - d\rho(\kappa,x) \, j2\kappa\sqrt{\varepsilon(x)} \; dx$$

where j is $\sqrt{-1}$.

Neglecting $dx d\Gamma$ and $d\rho(\kappa,x)dx$ terms gives

$$\rho(\kappa,x) + [\rho(\kappa,x)]^2 \, d\Gamma =$$

$$d\Gamma + \rho(\kappa,x) + d\rho(\kappa,x) - \rho(\kappa,x) \, j2\kappa\sqrt{\varepsilon(x)} \; dx$$

or

$$d\rho(\kappa,x) + \{1 - [\rho(\kappa,x)]^2\} \, d\Gamma$$
$$- \rho(\kappa,x) \, j2\kappa\sqrt{\varepsilon(x)} \; dx = 0 \tag{15}$$

Substituting Equation 12 into Equation 15 gives

$$d\rho(\kappa,x) - \left\{1 - [\rho(\kappa,x)]^2\right\} \frac{d\varepsilon(x)}{4\varepsilon(x)}$$
$$- \rho(\kappa,x) \, j2\kappa\sqrt{\varepsilon(x)} \, dx = 0$$

or

$$\frac{d\rho(\kappa,x)}{dx} - \frac{1}{4\varepsilon(x)} \{1 - [\rho(\kappa, x)]^2\} \frac{d\varepsilon(x)}{dx}$$
$$- \rho(\kappa, x) \, j2\kappa\sqrt{\varepsilon(x)} = 0 \tag{16}$$

Equation 16 is the Riccati nonlinear differential equation. The common solution of Equation 16 is given in Ulaby, Moore, and Fung (1981 as

$$\rho(\kappa,x) = -\int_{x}^{\infty} \frac{1 - [\rho(\kappa,s)]^2}{4\varepsilon(s)}$$

$$\cdot \frac{d\varepsilon(s)}{ds} e^{-j2\kappa \left[\int_0^s \sqrt{\varepsilon(u)} \, du - \int_0^x \sqrt{\varepsilon(u)} \, du \right]} ds \qquad (17)$$

When $x = 0$, the frequency domain reflection coefficient of the medium is

$$\rho(\kappa) = -\int_{0}^{\infty} \frac{1 - [\rho(\kappa,s)]^2}{4\varepsilon(s)}$$

$$\cdot \frac{d\varepsilon(s)}{ds} e^{-j2\kappa \left[\int_0^s \sqrt{\varepsilon(u)} \, du \right]} ds \qquad (18)$$

In Equation 18 $\rho(\kappa) = \rho(\kappa,0)$, which is a measurable boundary condition. Neglecting the $[\rho(\kappa,x)]^2$ term in Equation 18 gives the following equation

$$\rho(\kappa) \approx -\int_{0}^{\infty} \frac{1}{4\varepsilon(s)} \cdot \frac{d\varepsilon(s)}{ds} e^{-j2\kappa \left[\int_0^s \sqrt{\varepsilon(u)} \, du \right]} ds \qquad (19)$$

Now the following transformation is introduced:

$$y = 2\int_{0}^{s} \sqrt{\varepsilon(u)} \, du \qquad (20)$$

then

$$\frac{dy}{ds} = 2\sqrt{\varepsilon(s)} \qquad (21)$$

Using this transformation in Equation 19 produces the following is the result

$$\rho(\kappa) \approx -\int_{0}^{\infty} \frac{1}{8\varepsilon(s)\sqrt{\varepsilon(s)}} \cdot \frac{d\varepsilon(s)}{ds} e^{-j\kappa y} \, dy \qquad (22)$$

Equation 22 is the Fourier transform of $\rho(\kappa)$. It is an approximate inversion formulation that will produce accurate results as long as the many assumptions used in its derivation are valid. Disregarding the higher order infinitesimals such as $(d\Gamma)^2$, $(d\Gamma)^4$, $d\rho d\Gamma$, $dx d\Gamma$, $d\rho(\kappa,x)dx$, and the term $[\rho(\kappa,x)]^2$ will affect the result of the inversion process when the physical meaning of all or one of these terms is violated. As a result a target identification process is produced that is contaminated with a high rate of false alarm.

Pseudospectral Legendre approach for solving inverse problems

This approach for solving inverse problems is based on the idea of relating collocation nodes to the structure of orthogonal polynomials. Here, polynomial approximations are used to construct unknown profiles. These constructions are made in terms of the profiles' values at Legendre-Gauss-Lobatto nodes.

Let $L_N(t)$, $-1 \leq t \leq 1$, denote the Legendre polynomial of order N. Then the Legendre-Gauss-Lobatto nodes are defined by $t_o = -1$, $t_N = 1$, and $t_m = the$ *zeros of* $L_N{}'(t)$; $1 \leq m \leq N - 1$ where $L_N{}'(t)$ denotes the first derivative of $L_N(t)$. No explicit formula of the nodes t_m; $1 \leq m \leq N - 1$ is available. However, they can be computed numerically. Consider a function $F(t)$ and let it be defined over the closed interval $[-1,1]$, its Nth order interpolating polynomial $F^N(t)$ is defined as follows

$$F^N(t) = \sum_{h=0}^{N} b_h \, \phi_h(t) \tag{23}$$

where

$$\phi_h(t) = \frac{1}{N(N+1)L_N(t_h)}$$
$$\cdot \frac{(t^2 - 1) \, L'_N(t)}{(t - t_h)}, \quad h = 0,1,\ldots,N, \tag{24}$$

are Lagrange polynomials of order h, with the property

$$\phi_h(t_j) = \delta_{hj} = \begin{cases} 0 & \textit{if } h \neq j \\ 1 & \textit{if } h = j \end{cases} \tag{25}$$

Therefore $F^N(t_h) = b_h$.

The derivative, $F'(t)$, of the function $F(t)$ at the collocation points is approximated by the value of the derivative, $F'^N(t)$, of the function $F^N(t)$ at the collocation points t_m. To find the first derivative of $F^N(t)$ at the collocation

points t_m, Equation 23 is differentiated. The result is a matrix multiplication given in Gottlieb, Hussaini, and Orszag (1984) as

$$F'^{N}(t_m) = \sum_{h=0}^{N} b_h \phi'_h(t_m) \qquad (26)$$

where

$$\phi'_h(t_m) = \begin{cases} \dfrac{L_N(t_m)}{L_N(t_h)} \cdot \dfrac{1}{t_m - t_h}, & m \neq h \\[2ex] \dfrac{N(N+1)}{4} & m = h = 0 \\[2ex] -\dfrac{N(N+1)}{4} & m = h = N \\[2ex] 0 & otherwise \end{cases} \qquad (27)$$

and for the approximation of the second derivative of the function $F(t)$ at the collocation points, using the same method yields the following:

$$\phi''_h(t_m) = -2 \frac{L_N(t_m)}{L_N(t_h)} \cdot \frac{1}{(t_m - t_h)^2}, \qquad (28)$$

$$1 \leq m,h \leq N - 1; \; m \neq h$$

$$\phi''_h(t_h) = -\frac{1}{3} \frac{N}{1 - t_h^2}, \; 1 \leq h \leq N - 1; \; m = h \qquad (29)$$

Polynomial interpolation based on Legendre-Gauss-Lobatto points is well behaved compared to that based on equally spaced points (Davis 1963). Let the operation of interpolation given in Equation 26 be I_N, i.e., $F^N(t) = I_N F(t)$. Clearly I_N is a linear operator on $C([-1,1])$, the Banach space of continuous, real-valued function on $[-1,1]$, with the property $I_N = I_N^2$. This space is equipped with the uniform norm

$$|F|_\infty = \sup_{-1 \leq t \leq 1} |F(t)|, \; F \in C([-1,1]) \qquad (30)$$

Since I_N is a linear operator with the property $I_N = I_N^2$, then I_N is a projection operator whose range is the space of all polynomials of a degree less than or equal to $N - 1$. Furthermore, I_N is a bounded operator on $C([-1,1])$ with

$$|I_N| = \sup_{-1 \le t \le 1} \sum_{j=0}^{N} |\phi_j(t)| < \infty \qquad (31)$$

It follows that (Askey 1972)

$$\lim_{N \to \infty} \int_{-1}^{1} |F^N(t) - F(t)|^p \, dt = 0 \qquad (32)$$

for any $F \in C([-1,1])$ and $1 \le p < \infty$. Using the L^p norm provides

$$\lim_{N \to \infty} |F^N(t) - F(t)|_{L^p(-1,1)} = 0 \qquad (33)$$

from which the following is deduced

$$\sup_N |F^N|_p \le \infty, \; \forall \, F \in C([-1,1]) \qquad (34)$$

Thus, if the interpolation operation is considered as a linear operation from $C([-1,1])$ to $L_p(-1,1)$ then, from the Banach-Steinhaus Theorem, it follows that there exists a constant $g > 0$, which depends only on p, such that

$$|F^N|_p \le g \, |F|_\infty \qquad (35)$$

which is an upper bound on the Nth order interpolating polynomial of the function $F(t)$.

The following results are taken from Gottlieb, Hussaini, and Orzag (1984) to show the accuracy of approximating $F'(t)$ by $F'^N(t)$ and $F(t)$ by $F^N(t)$.

a. *Theorem 1.* Let $F(t)$ have σ smooth derivatives for $-1 \le t \le 1$, and define

$$|F|_\sigma^2 = \sum_{h=0}^{N} \int_{-1}^{1} \left(\frac{d^h F}{dt^h} \right)^2 dt \qquad (36)$$

Then there is a constant M independent of $F(t)$ and N such that

$$\sum_{i=0}^{\mu} \sqrt{\sum_{j=0}^{N} \left[\frac{d^{i}F(t_j)}{dt^{i}} - \frac{d^{i}F^{N}(t_j)}{dt^{i}} \right]^2} \leq MN^{2\mu-\sigma}|F|_{\sigma}, \quad \sigma > 2\mu \tag{37}$$

b. *Theorem 2.* For all $F \in H^{s}(-1,1)$, $s \geq 0$, there exists a constant M independent of $F(t)$ and N such that

$$|F - F^{N}|_{H^{q}(-1,1)} \leq MN^{[\sigma(q)-s]} |F|_{H^{s}(-1,1)}, \quad 0 \leq q \leq s \tag{38}$$

where $\sigma(q) = 2q - 1/2$.

Thus for a sufficiently smooth function, i.e., $F(t)$, the rate of convergence of $F'^{N}(t)$ to $F'(t)$ is faster than any power of $1/N$. This result serves as a basis for the convergence of the pseudospectral Legendre approach used for solving selected inverse problems in this report. The next theorem gives the error estimate in the supremum norm.

c. *Theorem 3.* If $t_0 = -1$, $t_N = 1$ and t_j, $1 \leq j \leq N - 1$ are the zeros of $L'_{N}(t)$ and $F(z)$ has no singularities except a finite number of poles, none of which lie on $[-1,1]$, and if for some n, $|F(z)/z^n| \to 0$ as $|z| \to \infty$, then $F^{N}(t) \to F(t)$ uniformly on $[-1,1]$.

Application of the Legendre-Gauss-Lobatto collocation method to the solution of inverse problems in dispersive media

In this section a numerical technique is proposed for solving the inverse problem in dispersive scattering theory. The inverse problem is first formulated as a relationship between the impulse response R and the susceptibility kernel G. The Legendre-Gauss-Lobatto nodes are used to construct the Nth polynomial interpolation to approximate the solution of G for a given R. This method is efficient and yields very accurate results. Examples are included to demonstrate the accuracy of this method.

When a radiation field interacts with an object, the scattered field carries information about the object's structure and composition. The inverse problem is posed by the retrieval of material parameters from measurements of a scattered field. Because of the complexity of the scattering interaction, reconstructed images of the scattering object obtained in real time are at best of dubious qualitative accuracy. In the context of electromagnetic (EM) scattering when the illuminated object is a lossless dielectric, accurate and quantitative inverse solutions are, as yet, available only for certain types of profiles (Moghaddam 1991). Most solutions are computationally intensive (Jordan and Ladouceur 1987) and are not attractive for real-time implementation.

In the case of electromagnetic wave propagation, the physical basis for the dispersive phenomenon lies in the following constitutive relationship (Jackson 1975)

$$D(x,t) = \varepsilon_0 \left[E(x,t) + \int_0^\infty G(s)E(x,t-s)\ ds \right] \tag{39}$$

In Equation 39, ε_0 is the permittivity of free space. Equation 39 is a relationship between the displacement field $D(x,t)$ at a point in a homogeneous medium, the susceptibility kernel G of the medium, and the past history of the electromagnetic field at that point, $E(x,s)$ for $-\infty < s \leq t$. The relationship between the susceptibility of the medium and its permittivity is given as (Beezley and Krueger 1985)

$$\frac{\varepsilon(\omega)}{\varepsilon_0} - 1 = \int_0^\infty G(t)e^{j\omega t}\ dt \tag{40}$$

where ω is the radial frequency. The inverse problem considered in this case involves determining the dispersive properties of a homogeneous medium, i.e., the susceptibility kernel G, by means of scattering methods. Here a direct computational method for solving this inverse problem is introduced. This approach is based on a spectral collocation method (pseudospectral method (Canuto et al. 1988)) in which N^{th} degree interpolating polynomials are constructed to approximate the susceptibility kernel. These polynomials are defined by using Legendre-Gauss-Lobatto points as the collocation points and Lagrange polynomials as the trial functions.

Problem formulation. Consider a homogeneous, isotropic, dispersive medium bounded by the planes $z = 0$ and $z = L > 0$. An electromagnetic plane wave is launched in the region $z < 0$. This impinges normally on the medium, giving rise to a left-moving reflected wave and a transient field within the medium. Assuming $E(z,t)$ denotes a transverse component of the electric field Equation 39 gives

$$E_{zz} - \frac{1}{c^2} \left[E_{tt} + \partial_t^2 \int_0^\infty G(s)E(z,t-s)\ ds \right] = 0,\ 0 < z < L \tag{41}$$

where $c^{-2} = \varepsilon_0\mu_0$, ε_0 and μ_0 being the permittivity and permeability of free space, respectively, and c is the speed of light. In the region $z < 0$, the field $E(z,t)$ can be split into

16

$$E(z,t) = E^+(z,t) + E^-(z,t) \tag{42}$$

where $E^+(z,t)$ and $E^-(z,t)$ are the incident and reflected fields respectively. The relationship between the incident and reflected fields is given in Beezley and Krueger (1985) as

$$E^-(z,t) = \int_0^\infty R(z,t-s)\, E^+(z,s)\, ds \tag{43}$$

where $R(z,t)$ is the impulse response. Using Equations 41-43 gives the following equation (Beezley and Krueger 1985):

$$2cR_z = 4R_t + G'(t) + G'(0)\,(2R + R * R) + G' \\ * (2R + R * R), \quad 0 < z < L, \quad 0 \leq t \leq T \tag{44}$$

$$R(L,t) = 0, \quad 0 \leq t \leq T \tag{45}$$

$$R(z,0^+) = -\frac{1}{4}\, G(0^+), \quad 0 < z < L \tag{46}$$

where T is the temporal length of the impulse response, $' = d/dt$ and the asterisk operation denotes a convolution in time;

$$R(z,t) * R(z,t) = \int_0^t R(z,u)\, R(z,t-u)\, du \tag{47}$$

In the special case of semi-infinite medium, $0 \leq z < \infty$, R is independent of z. Integrating Equation 44 with respect to t and using Equation 47 produces the following equation:

$$4R_1(t) + G(t) + 2G(t) * R_1(t) + G(t) * R_1(t) \\ * R_1(t) = 0, \quad 0 \leq t \leq T \tag{48}$$

In this case the solution of the inverse scattering problem is to obtain $G(t)$ for a given $R_1(t)$.

An approximation of the susceptibility function. In order to apply Legendre-Gauss-Lobatto nodes the following transformations are introduced:

$$z = \frac{1}{2} L (\beta + 1) \tag{49}$$

$$t = \frac{1}{2} T (\alpha + 1) \tag{50}$$

where the values of α and β are given on the interval $[-1,1]$. To solve Equation 44 the following approximation of $R(\beta,\alpha)$ and its derivatives are defined:

$$R^N (\beta,\alpha) = \sum_{i=0}^{N} \sum_{j=0}^{N} r_{ij} \phi_i (\beta) \phi_j (\alpha) \tag{51}$$

$$R_\beta^N (\beta,\alpha) = \sum_{i=0}^{N} \sum_{j=0}^{N} r_{ij} \phi'_i (\beta) \phi_j (\alpha) \tag{52}$$

where $\phi_i(\beta)$ and $\phi_j(\alpha)$ are trial functions as defined in Equation 24 and

$$R_\alpha^N (\beta,\alpha) = \sum_{i=0}^{N} \sum_{j=0}^{N} r_{ij} \phi_i (\beta) \phi'_j (\alpha) \tag{53}$$

The approximation of $G(\alpha)$ and its derivative are defined as

$$G^N(\alpha) = \sum_{i=0}^{N} g_i \phi_i (\alpha) \tag{54}$$

$$G'^N(\alpha) = \sum_{i=0}^{N} g_i \phi'_i (\alpha) \tag{55}$$

Using Equations 51-55, Equation 44 reduces to

$$\frac{4c}{L} R_\alpha^N = \frac{8}{T} R_\alpha^N + \frac{2}{T} G'^N + G(-1)$$
$$[2R^N + R^N * R^N] + G'^N * \left[\frac{4}{T} R^N + \frac{2}{T} R^N * R^N \right] \tag{56}$$

At the Legendre-Gauss-Lobatto nodes β_n, $n = 0, 1, 2,\ldots\ldots, N$, Equation 56 reduces to

18

$$\frac{4c}{L} \sum_{i=0}^{N} \sum_{j=0}^{N} r_{ij} \phi'_j (\beta_n) \phi_j (\alpha) = \frac{8}{T} \sum_{j=0}^{N} r_{nj} \phi'_j (\alpha)$$

$$+ \frac{2}{T} \sum_{i=0}^{N} g_i \phi'_i (\alpha) + 2g_0 \sum_{j=0}^{N} r_{nj} \phi_j (\alpha)$$

$$+ g_0 \sum_{i=0}^{N} \sum_{j=0}^{N} r_{ni} r_{nj} \int_0^t \phi_i (v) \phi_j (\alpha - v) \, dv$$

$$+ \frac{4}{T} \sum_{i=0}^{N} \sum_{j=0}^{N} g_i r_{nj} \int_0^t \phi'_i (v) \phi_j (\alpha - v) \, dv$$

$$\frac{2}{T} \sum_{i=0}^{N} \sum_{k=0}^{N} \sum_{j=0}^{N} g_i r_{nk} r_{nj}$$

$$\times \left[\phi'_i (\alpha) * \int_0^t \phi_k (v) \phi_j (\alpha - v) \, dv \right]$$

(57)

where v is a dummy variable. For a given $R(-1,\alpha)$, $0 \le i \le N$, Equation 57 is used to generate a set of nonlinear equations. This set of nonlinear equations is solved; as a result the coefficients g_i, $I = 0, 1,...., N$ are generated, and using Equation 54, the solution of the inverse problem can be calculated. In the special case of semi-infinite medium, let $Q(t) = R_1(t) * R_1(t)$, and $q = \frac{1}{2} T$ $(\theta + 1)$ where the value of θ is given on the interval $[-1,1]$. Using Equation 48, the following is the result

$$4R_1 \left(\frac{T}{2} (\alpha + 1) \right) + G \left(\frac{T}{2} (\alpha + 1) \right) + T$$

$$\int_{-1}^{(2t/T)-1} G \left(\frac{T}{2} (\theta + 1) \right) R_1 \left(t - \frac{T}{2} (\theta + 1) \right) d\theta$$

(58)

$$\frac{T}{2} \int_{-1}^{(2t/T)-1} G \left(\frac{T}{2} (\theta + 1) \right) Q \left(t - \frac{T}{2} (\theta + 1) \right) d\theta = 0$$

At $\alpha = t_k$, $k = 0, 1, 2,......, N$,

$$4R\left(\frac{T}{2}(t_k + 1)\right) + g_k + T \sum_{m=0}^{N} \frac{g_m}{N(N+1)L_N(t_k)}$$

$$\times \int_{-1}^{t_k} \left[\frac{(\theta^2 - 1) L'_n(\theta)}{\theta - t_m}\right] \cdot \left[R\left(\frac{T}{2}(t_k - \theta)\right)\right.$$

$$\left. + \frac{1}{2} Q\left(\frac{T}{2}(t_k - \theta)\right)\right] d\theta = 0 \tag{59}$$

Equation 59 is an algebraic equation that can be solved for the unknowns g_i, $i = 0, 1, 2,..., N$.

Numerical examples. This Legendre-Gauss-Lobatto nodes method is applied to solve two examples. In both examples the impulse response is known, whereas $G(t)$ needs to be estimated. For the purpose of this demonstration the direct problem had to be solved in order to generate $R(0,t)$. This function then is used to solve the inverse problem and generate the corresponding $G(t)$.

    a.   *Example 1.* A two-resonance model for the electron contribution to the permittivity is used in this example. Thus G is given by (Beezley and Krueger 1985)

$$G(t) = e^{-0.2t} \sin(1.6\pi t) + 0.5e^{-0.5t} \sin(6\pi t) \tag{60}$$

The depth of the medium is taken as $L = 0.8$ and the chosen time $T = 6$. The approximate value of the unknown function, i.e., $G^N(t_n)$, is calculated for $N = 4$. In Table 1, the values of the approximate and exact susceptibility function at the Legendre-Gauss-Lobatto nodes are reported.

Table 1
Results of Example 1

t_n $0 \leq n \leq 4$	$G^4(t_n)$	$G(t_n)$
-1.000000	0.0014	0
-0.654654	-0.4799	-0.4808
0	0.3228	0.3226
0.654654	-0.0992	-0.0996
1.000000	-0.2855	-0.2864

b. *Example 2.* In this example the medium is semi-infinite; the impulse response is taken as $R_1(t) = t$, and the time is taken as $T = 10$. The exact solution for $G(t)$ is given as

$$G(t) = -2 \; (\sin t + t \cos t) \tag{61}$$

The approximate and exact susceptibility functions at the Legendre-Gauss-Lobatto nodes for $N = 8$ are given in Table 2.

Table 2
Results of Example 2

t_n $0 \leq n \leq 6$	$G^8(t_n)$	$G(t_n)$
-1.000000	0.0012	0
-0.899757	-1.8410	-1.8401
-0.677186	-1.8495	-1.8584
-0.363117	6.4341	6.4486
0	-0.9205	-0.9187
0.363117	-12.7680	-12.7597
0.677186	6.7687	6.7832
0.899757	19.1291	19.0935
1.000000	17.8995	17.8695

Application of the Legendre-Gauss-Lobatto collocation method to Gel'fand-Levitan integral equation

One way to solve a one-dimensional inverse scattering problem is through the Gel'fand-Levitan integral equation. The closed-form solution of this integral equation is not easy to obtain. In this section a numerical method for solving this integral equation is proposed, hence an alternative method of construction of arbitrary dielectric profiles. Two examples are given to demonstrate the accuracy of this method. Pioneering work in this subject was performed by Gel'fand and Levitan (1955), Marchenko (1955), and Kay (1955, 1960). These authors determined the scattering potential associated with the time-independent Schrödinger equation from scattering data, such as reflection and transmission coefficients. The Gel'fand-Levitan integral equation is a formulation of an inverse problem. However, explicit solutions of this equation are seldom easy to obtain (Kritikos, Jaggard, and Ge 1982). Solutions for the Gel'fand-Levitan integral equation have been constructed by Kritikos, Jaggard, and Ge (1982), Jordan and Ladouceur (1987), Kay (1960), and Reilly and Jordan (1981). Recent approximate methods of solving inverse problems

are given in Cui and Liang (1994a, 1995), Razzaghi and Ahmad (1995), and Kincanon (1993).

Problem formulation. The Gel'fand-Levitan approach is based on the solution of the following integral equation (Kritikos, Jaggard, and Ge 1982):

$$R(z + y) + K(z,y) + \int_{-y}^{z} K(z,z') R(y + z') dz' = 0$$

$$z \geq 0$$

$$-z \leq y \leq z$$

(62)

where $K(z,y)$ is the kernel and $R(z + y)$ is the transformed reflection coefficient. The dielectric permittivity, $\varepsilon(z)$, is related to the potential function, $v(z)$, through the following relationship (Kritikos, Jaggard, and Ge (1982)):

$$\varepsilon(z) = 1 - v(z)/\kappa^2$$

(63)

The solution for the potential function produces the following equalities (Gel'fand and Levitan 1955; Kay 1960):

$$v(z) = \begin{cases} 2dK(z,z)/dz, & z \geq 0 \\ 0, & z < 0 \end{cases}$$

(64)

$$[\partial^2 K(z,y)/\partial z^2] - [\partial^2 K(z,y)/\partial y^2]$$
$$- [2K(z,y) \; \partial K(z,z)/\partial z] = 0$$

(65)

$$R(z) = 0, \; z < 0$$

(66)

The aim is to solve for the permittivity $\varepsilon(z)$. Substituting the solution of Equation 65 in Equation 64 and making use of Equation 63 an expression for $\varepsilon(z)$ is produced.

An approximation of the dielectric profile. In order to apply Legendre-Gauss-Lobatto nodes the following transformations are introduced

$$z = \frac{z_1}{2} (\alpha + 1) - \frac{z_2}{2} (\alpha-1)$$

(67)

$$y = \frac{y_1}{2} (\beta + 1) - \frac{y_2}{2} (\beta - 1) \qquad (68)$$

where z_1, z_2, y_1 and y_2 are the limits of z and y. The values of α and β are in the interval $[-1,1]$. Define the approximation of $K(z,y)$ and its derivatives as follows:

$$K^N (\alpha,\beta) = \sum_{i=0}^{N} \sum_{j=0}^{N} a_{ij} \, \phi_i(\alpha) \, \phi_j(\beta) \qquad (69)$$

$$K_\alpha^N (\alpha,\beta) = \sum_{i=0}^{N} \sum_{j=0}^{N} a_{ij} \, \phi_i'(\alpha) \, \phi_j(\beta) \qquad (70)$$

$$K_\beta^N (\alpha,\beta) = \sum_{i=0}^{N} \sum_{j=0}^{N} a_{ij} \, \phi_i(\alpha) \, \phi_j'(\beta) \qquad (71)$$

Using Equations 67 and 68, Equation 65 takes the following form:

$$\left(\frac{2}{L}\right)^2 \frac{\partial^2 K(\alpha,\beta)}{\partial \alpha^2} - \left(\frac{2}{L}\right)^2 \frac{\partial^2 K(\alpha,\beta)}{\partial \beta^2}$$
$$- 2K(\alpha,\beta)\left(\frac{2}{L}\right)\frac{\partial K\,(\alpha,\alpha)}{\partial \alpha} = 0 \qquad (72)$$

where $L = z_2 - z_1 = y_2 - y_1$. Using Equations 69-71, Equation 72 is reduced to

$$\sum_{i=0}^{N} \sum_{j=0}^{N} a_{ij} \, \phi_i''(\alpha) \, \phi_j(\beta) - \sum_{i=0}^{N} \sum_{j=0}^{N}$$
$$a_{ij} \, \phi_i(\alpha) \, \phi_j''(\beta) - L \, K^N (\alpha,\beta) \sum_{i=0}^{N} \sum_{j=0}^{N} \qquad (73)$$
$$a_{ij} \, [\phi_i(\alpha) \, \phi_j(\alpha)]' = 0$$

At the Legendre-Gauss-Lobatto nodes $\alpha = \alpha_n$ and $\beta = \beta_m$, Equation 73 reduces to

$$\sum_{i=0}^{N} a_{im} \phi_i{}'' (\alpha_n) - \sum_{j=0}^{N} a_{nj} \phi_j{}'' (\beta_m)$$

$$- L a_{nm} \left[\sum_{j=0}^{N} a_{nj} \phi_j{}' (\alpha_n) + \sum_{i=0}^{N} a_{in} \phi_i{}' (\alpha_n) \right] = 0 \tag{74}$$

The unknowns in Equation 74 are the coefficients a_{ij}; $I, j = 0, 1, 2,..., N$. In order to solve for the unknown coefficients, the following conditions will be used. Differentiating Equation 62 gives

$$\frac{\partial R(z + y)}{\partial y} + \frac{\partial K(z,y)}{\partial y} +$$

$$\int_{-y}^{z} K(z,z') \frac{\partial R(y + z')}{\partial y} dz' + K(z,-y) R(0) = 0 \tag{75}$$

and

$$\frac{\partial^2 R(z + y)}{\partial y^2} + \frac{\partial^2 K(z,y)}{\partial y^2} + \int_{-y}^{z} K(z,z')$$

$$\frac{\partial^2 R(y + z')}{\partial y^2} dz' + K(z,-y) \tag{76}$$

$$\frac{\partial R(y + z')}{\partial y}\bigg|_{z' = -y} + \frac{\partial K(z,-y)}{\partial y} R(0) = 0$$

Let $z = -y$, Equations 75 and 76 reduce to

$$\frac{\partial R(z + y)}{\partial y}\bigg|_{z = -y} + \frac{\partial K(z,y)}{\partial y}\bigg|_{z = -y} + K(z,z) R(0) = 0 \tag{77}$$

and

$$\left.\frac{\partial^2 R(z+y)}{\partial y^2}\right|_{z=-y} + \left.\frac{\partial^2 K(z,y)}{\partial y^2}\right|_{z=-y}$$
$$+\, K(z,z)\left.\frac{\partial R(y+z')}{\partial y}\right|_{z'=z} + \left.\frac{\partial K(z,-y)}{\partial y}\right|_{z=-y} R\,(0) = 0 \tag{78}$$

Equations 77 and 78 are two conditions under which Equation 74 is solved. As a special case when $R(0) = 0$

$$\left.\frac{\partial R(z+y)}{\partial y}\right|_{z=-y} + \left.\frac{\partial K(z,y)}{\partial y}\right|_{z=-y} = 0 \tag{79}$$

and

$$\left.\frac{\partial^2 R(z+y)}{\partial y^2}\right|_{z=-y} + \left.\frac{\partial^2 K(z,y)}{\partial y^2}\right|_{z=-y}$$
$$+\, K(z,z)\left.\frac{\partial R(y+z')}{\partial y}\right|_{z'=z} = 0 \tag{80}$$

Also from Equation 62

$$K\,(z,-z) = 0 \tag{81}$$

As $n, m = 0, 1, 2, 3,..., N$, Equation 74 reduces to a set of nonlinear algebraic equations. Solving this set of equations results in values for the unknown coefficients. The initial value of the potential function is deduced from Equations 62 and 64. Its final expression is

$$v(0) = -2\left.\frac{\partial R\,(2z)}{\partial z}\right|_{z=0} \tag{82}$$

Numerical examples. Two examples of inverse problems are selected and solved to test the numerical scheme proposed in this section. The first example was considered in Kritikos, Jaggard, and Ge (1982). It was solved numerically through an iterative method. The second example was considered in Moses and de Ridder (1963) and solved analytically. Given the complex

25

reflection coefficient, $r(\kappa)$, the requirement in both examples is to reconstruct the dielectric profile as a function of depth, i.e., $\varepsilon(z)$. As it is seen from Equation 63, this requirement is translated to reconstructing the potential function $v(z)$.

a. *Example 1.* As a result of a test, the reflection coefficient is given as

$$r(\kappa) = \frac{-k_1 \, k_2}{(\kappa - k_1) \, (\kappa - k_2)} \tag{83}$$

where

$$k_1 = \frac{(1 - j)}{\sqrt{2}}$$

and

$$k_2 = \frac{-(1 + j)}{\sqrt{2}}$$

The transform of $r(\kappa)$ is (Kritikos, Jaggard, and Ge 1982)

$$R(z) = \frac{-j}{\sqrt{2}} \left[e^{\frac{-z\,(1 + j)}{\sqrt{2}}} - e^{\frac{-z\,(1 - j)}{\sqrt{2}}} \right] \tag{84}$$

This example is treated in the area bounded by $0 \leq z \leq 0.5$ and $0 \leq y \leq 0.5$. The exact and approximate values of the function $v(z)$ are given in Table 3.

Table 3 Values of the Function $v(z)$, Example 1		
z	Approximate $v(z)$	Exact $v(z)$
0.00000	4.00000	4.00000
0.08634	3.17540	3.17686
0.25000	2.18449	2.18328
0.41366	1.59203	1.59220
0.50000	1.37141	1.37258

b. *Example 2.* The reflection coefficient from testing a certain dielectric medium is given as

$$r(\kappa) = \frac{-k_1 k_2}{(\kappa - k_1)(\kappa - k_2)} \qquad (85)$$

where

$$k_1 = j$$
$$\text{and}$$
$$k_2 = -j$$

The transform of $r(\kappa)$ is (Moses and deRidder 1963)

$$r(z) = Sinh\ (z) \qquad (86)$$

This example is also treated in the area bounded by $0 \le z \le 0.5$ and $0 \le y \le 0.5$. The exact and approximate values of the function v(z) are given in Table 4.

Table 4
Values of the Function $v(z)$

z	Approximate v(z)	Exact v(z)
0.00000	-4.00000	-4.00000
0.08634	-3.94063	-3.94096
0.25000	-3.53830	-3.53890
0.41366	-2.89300	-2.89205
0.50000	-2.51071	-2.51716

Application of the Legendre-Gauss-Lobatto collocation method to Zakharov-Shabat equations

This is a case in which a numerical method is proposed to solve the inverse scattering problem associated with two Gel'fand-Levitan-Marchenko integral equations. This inverse problem is represented by two coupled partial differential equations. The solution of these partial differential equations is two kernel functions. These kernels are also related to each other through the Gel'fand-Levitan-Marchenko integral equations. Legendre-Gauss-Lobatto nodes are used to construct the Nth polynomial interpolation to approximate the solution of the kernel functions related to the scattering potential. Zakharov-Shabat equations are used to formulate inverse scattering problems in Frangos and Jaggard (1991, 1992). Gel'fand-Levitan-Marchenko coupled integral equations are associated with the Zakharov-Shabat equations (Lamb 1980). Applications of the solution of these types of inverse scattering problems are presented in Song and Shin (1985).

Again, this numerical approach is based on a spectral collocation method given in Canuto et al. (1988). In this numerical approach, N^{th} degree interpolating polynomials are constructed to approximate the kernels, which in turn are related to the scattering potential. These polynomials are defined through the use of Legendre-Gauss-Lobatto points as collocation points and Lagrange polynomials as trial functions.

Problem formulation. The linear two-component Zakharov-Shabat coupled equations are given in Lamb (1980) as

$$\frac{dv_1(x,\kappa)}{dx} + i\kappa v_1(x,\kappa) = q(x)v_2(x,\kappa) \tag{87}$$

$$\frac{dv_2(x,\kappa)}{dx} - i\kappa v_2(x,\kappa) = -q^*(x)v_1(x,\kappa) \tag{88}$$

where

$$v_1(x,\kappa), v_2(x,\kappa) = \text{modes of propagation}$$

$$q(x) = \text{potential function}$$

and the asterisk denotes conjugation. In this case x represents depth in the medium in which the propagation is taking place. As a solution of this inverse problem, given the reflection coefficient, $r(\kappa)$, it is desired to find the function $q(x)$. $r(\kappa)$ is the ratio of the reflected and incident electric fields. It is shown in Lamb (1980) that in the region $x > y$ Equations 87 and 88 are related to two Gel'fand-Levitan-Marchenko coupled integral equations. These integral equations are

$$A_1^*(x,y) + \int_{-y}^{x} A_2(x,t)R(y + t)\ dt = 0 \tag{89}$$

$$- A_2^*(x,y) + R(x + y) + \int_{-y}^{x} A_1(x,t)R(y + t)\ dt = 0 \tag{90}$$

where $A_1(x,y)$ and $A_2(x,y)$ are the kernels and $R(x)$ is the Fourier transform of the reflection coefficient $r(\kappa)$. In region $x>y$ the relationships between the two kernels $A_1(x,y)$ and $A_2(x,y)$ are given in Lamb (1980) as

28

$$\frac{\partial A_1(x,y)}{\partial y} + \frac{\partial A_1(x,y)}{\partial x} = q(x)A_2(x,y) \tag{91}$$

$$\frac{\partial A_2(x,y)}{\partial y} - \frac{\partial A_2(x,y)}{\partial x} = q^*(x)A_1(x,y) \tag{92}$$

where

$$q^*(x) = -2A_2(x,x)$$

and

$$|q(x)|^2 = -2\frac{dA_1(x,x)}{dx}$$

From Equations 89 and 90, in the limit $y \rightarrow -x$

$$A_1^*(x,-x) = 0 \tag{93}$$

$$A_2^*(x,-x) = R(0) \tag{94}$$

Differentiating Equations 89 and 90 and letting $y \rightarrow -x$

$$\left.\frac{\partial A_1^*(x,y)}{\partial y}\right|_{y=-x} + A_2(x,x)R(0) = 0 \tag{95}$$

$$-\left.\frac{\partial A_2^*(x,y)}{\partial y}\right|_{y=-x} + \left.\frac{\partial R(x+y)}{\partial y}\right|_{y=-x} \\ + A_1(x,x)R(0) = 0 \tag{96}$$

Equations 93-96 are conditions under which Equations 91 and 92 are solved and solutions for the two kernels $A_1(x,y)$ and $A_2(x,y)$ are generated. Consequently, a solution for the potential function $q(x)$ is produced.

An approximation of the potential function. In order to be able to apply Legendre-Gauss-Lobatto nodes and solve the inverse problem, consider the following transformations:

$$x = \frac{L}{2} (1 + \alpha) \tag{97}$$

$$y = \frac{L}{2} (1 + \beta) \tag{98}$$

where L is the range of x. The values of α and β are in the interval $[-1,1]$. Define the approximations of the kernels $A_1(x,y)$ and $A_2(x,y)$ as

$$A_1^N (\alpha,\beta) = \sum_{i=0}^{N} \sum_{j=0}^{N} \gamma_{ij} \, \phi_i (\alpha) \, \phi_j (\beta) \tag{99}$$

$$A_2^N (\alpha,\beta) = \sum_{i=0}^{N} \sum_{j=0}^{N} \zeta_{ij} \, \phi_i (\alpha) \, \phi_j (\beta) \tag{100}$$

where γ and ζ are two coefficients and the function ϕ is given in Equation 24. From the definition of $q^*(x)$ (following Equation 92)

$$q^N(\alpha) = -2 \sum_{i=0}^{N} \sum_{j=0}^{N} \zeta_{ij}^* \, \phi_i (\alpha) \, \phi_j (\alpha) \tag{101}$$

The differentiations of Equation 99 with respect to α and β are

$$A_1^N(\alpha,\beta)_\alpha = \sum_{i=0}^{N} \sum_{j=0}^{N} \gamma_{ij} \, \phi_i' (\alpha) \, \phi_j (\beta) \tag{102}$$

$$A_1^N(\alpha,\beta)_\beta = \sum_{i=0}^{N} \sum_{j=0}^{N} \gamma_{ij} \, \phi_i (\alpha) \, \phi_j' (\beta) \tag{103}$$

Equations similar to Equations 102 and 103 can be generated from Equation 100.

Application of Equations 99 and 100 and their corresponding derivatives to Equations 91 and 92 results in the following equations

$$\sum_{i=0}^{N} \sum_{j=0}^{N} \gamma_{ij} \, \phi_i(\alpha) \, \phi_j'(\beta) + \sum_{i=0}^{N} \sum_{j=0}^{N} \gamma_{ij} \, \phi_i'(\alpha) \, \phi_j(\beta)$$

$$= -L \left[\sum_{i=0}^{N} \sum_{j=0}^{N} \zeta_{ij}^* \, \phi_i(\alpha) \, \phi_j(\alpha) \right] \tag{104}$$

$$\cdot \left[\sum_{i=0}^{N} \sum_{j=0}^{N} \zeta_{ij} \, \phi_i(\alpha) \, \phi_j(\beta) \right]$$

$$\sum_{i=0}^{N} \sum_{j=0}^{N} \zeta_{ij} \, \phi_i(\alpha) \, \phi_j'(\beta) - \sum_{i=0}^{N} \sum_{j=0}^{N} \zeta_{ij} \, \phi_i'(\alpha) \, \phi_j(\beta)$$

$$= -L \left[\sum_{i=0}^{N} \sum_{j=0}^{N} \zeta_{ij} \, \phi_i(\alpha) \, \phi_j(\alpha) \right] \tag{105}$$

$$\cdot \left[\sum_{i=0}^{N} \sum_{j=0}^{N} \gamma_{ij} \, \phi_i(\alpha) \, \phi_j(\beta) \right]$$

Considering the case where $R(x)$ is real, at the Legendre-Gauss-Lobatto nodes $\alpha = \alpha_n$ and $\beta = \beta_m$ Equations 104 and 105 reduce to

$$\sum_{j=0}^{N} a_{nj} \, \phi_j'(\beta_m) + \sum_{i=0}^{N} a_{im} \, \phi_i'(\alpha_n) = -L \, c_{nn} \cdot c_{nm} \tag{106}$$

$$\sum_{j=0}^{N} c_{nj} \, \phi_j'(\beta_m) - \sum_{i=0}^{N} c_{im} \, \phi_i'(\alpha_n) = -L \, c_{nn} \cdot a_{nm} \tag{107}$$

where a and c are the real parts of the coefficients γ and ζ. As $n, m = 0, 1, 2, ..., N$ two sets of algebraic equations are generated. Solution of these algebraic equations results in values for the coefficients a and c. Consequently, from Equation 101 the potential function $q(x)$ is known at the Legendre-Gauss-Lobatto nodes.

A numerical example. Let the reflection coefficient be given as

$$r(\kappa) = \frac{1}{2} \frac{j}{(\kappa + j)} \tag{108}$$

The Fourier transform of $r(\kappa)$ is

$$R(x) = \frac{1}{2} e^{-x} \tag{109}$$

The exact expression for the corresponding potential function is given in Frangos and Jaggard (1991) as

$$q(x) = \frac{2s\,(1 - s)}{(s - 1)^2\, e^{-2sx} + \frac{1}{4}\, e^{2sx}}$$

(110)

where $s = 1.11803399$. The Legendre-Gauss-Lobatto method was used to solve this inverse scattering problem and generate the corresponding potential function numerically. The computations were carried out for $N = 4$ and $N = 6$. Results from these computations are presented in Tables 5 and 6.

The first column in Tables 5 and 6 shows the Legendre-Gauss-Lobatto nodes. The second column shows the values of the computed potential function, and the third column shows the corresponding exact values.

Table 5
Estimated and Exact Values of $q(\alpha)$ with $N = 4$

α_n $0 \leq n \leq 4$	$q^4(\alpha_n)$	$q(\alpha_n)$
-1.000000	-1.0000000	-1.0000000
-0.654654	-0.4776921	-0.4820000
0.000000	-0.1124612	-0.1127600
0.654654	-0.0257691	-0.0261026
1.000000	-0.0119132	-0.0120594

Table 6
Estimated and Exact Values of $q(\alpha)$ with $N = 6$

α_n $0 \leq n \leq 6$	$q^6(\alpha_n)$	$q(\alpha_n)$
-1.00000000	-1.00000000	-1.00000000
-0.83022390	-0.70289322	-0.70388000
-0.46884879	-0.32025671	-0.32025800
0.00000000	-0.11274966	-0.11276200
0.46884879	-0.03953648	-0.03954590
0.83022390	-0.01758667	-0.01762760
1.00000000	-0.01207034	-0.01205940

Effect of Noise on the Pseudospectral Legendre Method Applied for Solving Inverse Problems

A criterion for the effect of noise on the Legendre-Gauss-Lobatto pseudo-spectral method is formulated in this section. For the purpose of demonstration a particular inverse problem is utilized. Consider the inverse problem of a semi-infinite scattering medium in the region $z > 0$, in which the velocity profile $c(z)$ is arbitrary, with $c(z)$ constant in $z < 0$. The gradient-type interface at $z = 0$ is characterized by a jump in the first derivative of $c(z)$, i.e., c_z. In addition, $c(z)$ itself is continuous everywhere, while c_z is continuous everywhere except at the interface. The form of the wave equation used here is (Kreider 1989)

$$u_{zz}(z,t) - c^{-2}(z)u_{tt}(z,t) = 0 \tag{111}$$

Introducing the travel time coordinate x

$$x(z) = \int_0^z da/c \ (a) \tag{112}$$

Equation 111 takes the following form

$$v_{xx}(x,t) - v_{tt}(x,t) - b(x)v_x \ (x,t) = 0 \tag{113}$$

where

$$v(x,t) = u(z,t)$$

and

$$b(x) = c_z(z)$$

Given some knowledge of the electromagnetic field, the solution of this inverse problem is to reconstruct the velocity profile, i.e., $c(z)$, starting from the interface up to a specified distance into the medium, i.e., Z. The strategy is to let a known right-moving incident wave propagate from $z = -\infty$ so that it impinges upon the inhomogeneous medium beginning at time $t = 0$. The impulse response of the medium, $r \ (x,t)$, satisfies the following equation

$$r_x(x,t) - 2r_t(x,t) = \frac{1}{2} b(x) \, r * r \qquad (114)$$

with initial condition

$$r(x,0) = \frac{1}{4} b(x) \qquad (115)$$

where the asterisk denotes a convolution in time. In addition the following integral is defined

$$L = \int_0^Z da/c(a) \qquad (116)$$

For a given $r(0,t)$, one can apply the formulated Legendre-Gauss-Lobatto collocation method and solve this inverse problem. The question is how this method will behave when the function $r(0,t)$ is contaminated with noise. To answer this question, consider the following criteria:

a. Let the noise be additive. Accordingly the following equation

$$\hat{r}(0,t) = r(0,t) + n(t) \qquad (117)$$

represents the contaminated impulse response where $n(t)$ is the additive noise.

b. $n(t)$ may take many statistical shapes. Distribution functions may be applied such as the Uniform, Arcsin, Beta, Cauchy, Chi-Square, Erlang, Exponential, Gamma, Gaussian, Laplace, Log-Normal, Rayleigh, Rice, or Weibull to represent the noise.

c. In every case, the contaminated impulse response given in Equation 117 is used as an input to the formulated Legendre-Gauss-Lobatto collocation method, and the corresponding velocity profile is generated.

d. Data generated from step c can be used to make comparisons and study the behavior of the formulated Legendre-Gauss-Lobatto collocation method in the presence of the different types of noise. The presence of one type should be exclusive.

e. Represent the root mean square of the signal-to-noise ratio as

34

$$rms\left[\frac{S}{N}\right] = \frac{\frac{1}{2}\int\limits_{-1}^{1}\sqrt{[r\,(-1,u)\,-\,\bar{r}\,]^2}\ du}{SD} \qquad (118)$$

where SD is the standard of deviation and

$$\bar{r} = \frac{1}{2}\int\limits_{-1}^{1}r\,(-1,s)\ ds \qquad (119)$$

3 Radar Employment

Some of the investigations described in this Chapter are laboratory procedures that will be discussed in a subsequent report. However, such procedures are mentioned here. Thus far in this report a formulated scheme for solving inverse problems is proposed. In this Chapter the design and criteria of a high-resolution radar are discussed. This radar is designed with the concept of its employment for the evaluation of inversion schemes. As discussed in the preceding Chapter, the input to the inversion processes that is selected for the application of the formulated Legendre-Gauss-Lobatto collocation method is the impulse response or complex reflection coefficient of the tested medium.

A network analyzer that is configured as a radar system will be used to generate the impulse response of a medium under testing. Characterization of the system's configurations is not within the scope of this report.

A high-resolution radar is designed to generate the complex reflection coefficient in the laboratory. This radar will be developed before the evaluation and testing of different formulated inversion schemes. This radar generates a specific carrier wave form. Its transmitted signal is composed of a coded version of this wave form. Barker codes are used in the encoding process. For convenience, the known Barker codes are listed in Table 7.

Table 7 The Known Barker Codes	
Length of code	Code Elements
1	+
2	+ - or + +
3	+ + - or + - +
4	+ + - + or + + + -
5	+ + + - +
7	+ + + - - + -
11	+ + + - - - + - - + -
13	+ + + + + - - + + - + - +

From Table 7, it is seen that Barker codes are binary codes with different lengths. As the radar is made operational, one code length is selected. Accordingly, the transmitted wave form from the radar is made of segments, the number of which is equal to that of the bits in the selected code. Here, the "+" and "-" signs of Barker code correspond to 0-deg and 180-deg phase angles, respectively. They are used to set the phase of each corresponding segment from the transmitted wave form. Take, for example, the application of Barker code of length 4, i.e., + + - +. The phases of the first, second and the fourth segments of the transmitted signal are set to 0 deg, and the phase of the third one is set to 180 deg. Thus Barker codes are phase codes. An onboard microprocessor is used to select the appropriate code length.

Let the duration of an uncoded transmitted radar signal be T. Then the range resolution, δ_r, of this signal is (Eaves and Reedy 1987)

$$\delta_r = \frac{c}{2B} = \frac{cT}{2} \tag{120}$$

where c is the speed of light and B is the bandwidth of the transmitted signal. It equals to $1/T$. The small value of δ_r implies that the radar can resolve small range values; therefore, it is a high-resolution radar. As it is seen from Equation 120, a high-resolution radar requires that B be very large, i.e., that T be very small, e.g., τ. This requirement leads to hardware complications. This important criterion can, however, be achieved through pulse compression techniques where the hardware implementation is much easier. In pulse compression the total duration of the uncoded transmitted radar signal is divided into N pulses. The duration of each pulse is selected to be τ. Accordingly, the pulse compression ratio, CR, is

$$CR = \frac{T}{\tau} \tag{121}$$

and the radar's range resolution is

$$\delta_r = \frac{c}{2B} = \frac{c\tau}{2} \tag{122}$$

It should be noted that the values of the bandwidth, B, in Equations 120 and 122 are different: it is larger in the latter. A pulse compression technique is implemented in the design of the high-resolution radar. In this case the transmitted signal is encoded using Barker codes as described previously and thus high resolution is achieved. Application of high-resolution radar includes object detection, target classification, train mapping, and as an aid in any

application in distributed clutter suppression (Eaves and Reedy 1987). Two operations are performed in the receiver of this high-resolution radar. In the first operation the complex reflection coefficient is generated as a ratio between the incident and reflected energies. In the second operation the baseband information is extracted from the reflected signal through envelope detection. Information from the first operation will be used as an input to schemes used to solve inverse problems under study. On the other hand, information generated from the second operation will show the changes in the signal's amplitude due to its propagation in the medium under testing.

An Improved Portable High-resolution Radar

In this section an improved portable high-resolution radar is proposed. Some information regarding this radar is presented.

Prior art

Up to the present time, all carriers used in radar technology have been sinusoidal signals. However, these carriers can be coded or not coded depending on the type of radar used. Codes used in high-resolution radar are Barker, Frank, Costas, and Welti, among others. For example, carriers of ground-penetrating radars are not coded. Most ground-penetrating radars are somewhat portable but not to the extent of being hand-held. In some ground-penetrating radars the antenna is designed to slide on the surface of the medium that is being tested. This action limits their applications. As another example, a synthetic aperture radar is a high-resolution radar; however, it is not a hand-held radar. This radar takes advantage of the forward motion of the airborne radar to produce the equivalent of an array antenna that may be thousands of feet long. Moreover, the beamwidth of this array is roughly half that of a real array of the same length. The outputs of the array are synthesized in a signal processor from the returns received by the real radar antenna over a period of up to several seconds or more.

The concept

The high-resolution radar system is designed to be hand-held, portable, and microprocessor controlled. The generated carrier is an exponentially decaying sinusoidal wave. The frequency of the carrier is in the GHz range. In this high-resolution radar, analog to digital conversion is performed through an integrated circuit chip at a rate of multiple gigasamples per second. In addition, digital signal processes are applied and inversion schemes are imbedded in memory chips to generate electromagnetic profiles in real time. In order to achieve high resolution, digital codes such as Barker, Welti, or Frank codes can easily be implemented in this radar system through the application of C^2MOS logic. The coding of the carrier is made possible through the

application of digitally controlled phase shifters. Power consumption of this high-resolution radar is moderate. Thus, in addition to being hand-held, the complete system is mountable on any vehicle as well. As a result, this radar system can be used to perform target and media identification in real time. This process is totally performed by the microprocessor in the system, and identification results are displayed visually.

System description

The portable high-resolution radar is of four parts: a transmitter, a receiver, a microprocessor, and d-c power supply.

a. *Transmitter.* A block diagram of the transmitter is shown in Figure 1. The transmitter includes the following items:

(1) A keypad.

(2) Shift registers.

(3) A carrier generating circuit.

(4) A phase shifter.
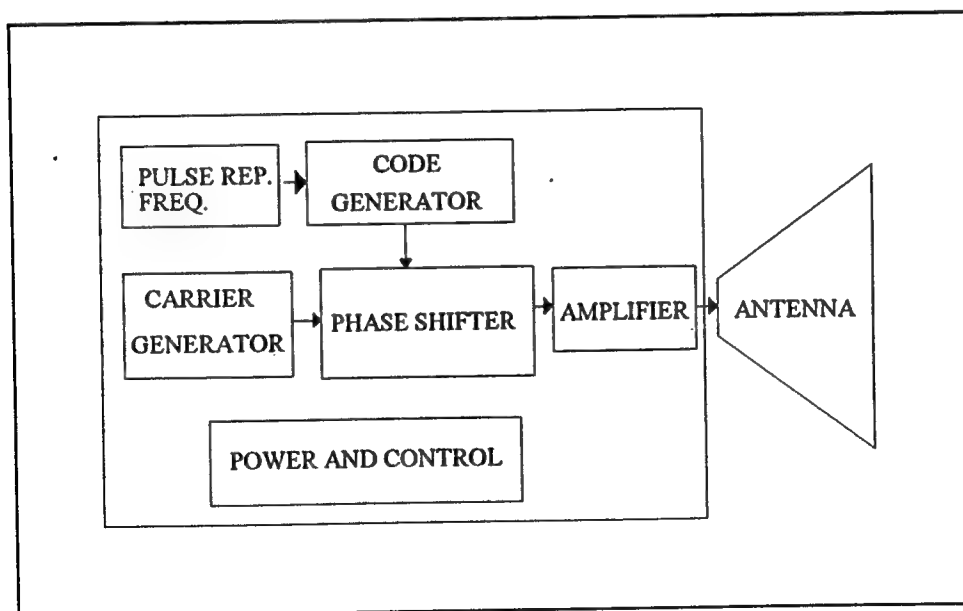
(5) A power amplifier.

(6) A transmitting antenna.

Figure 1. Transmitter

b. *Receiver.* A block diagram of the receiver is shown in Figure 2. The receiver includes the following items:

(1) A receiving antenna.

(2) An envelope detector.

(3) A circuit to generate the complex coefficient of reflection function.

(4) A circuit to perform inversion and generate electromagnetic profiles.

(5) An analog-to-digital convertor.
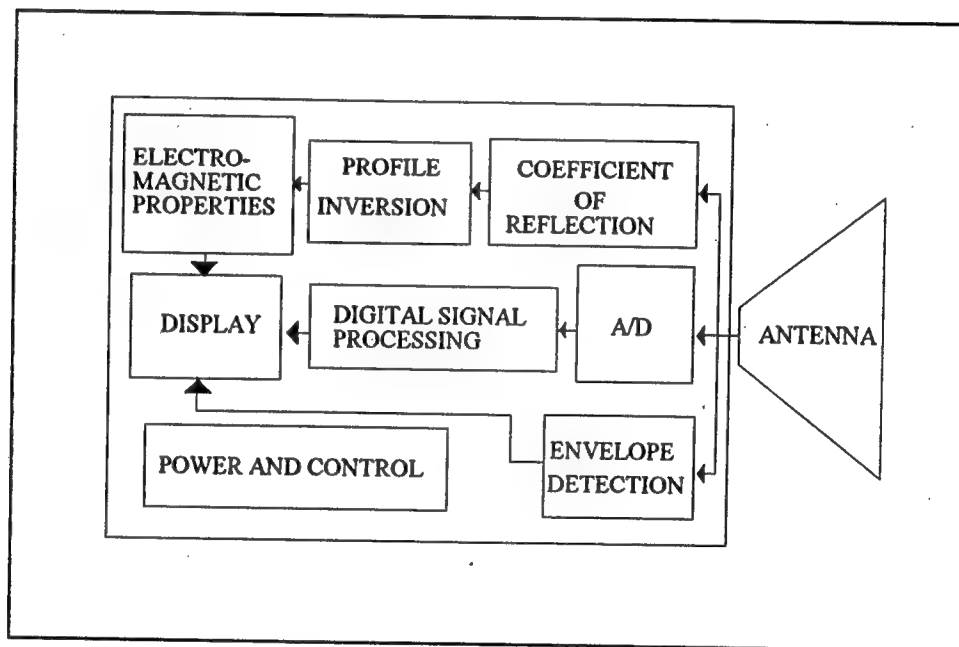
(6) A digital signal-processing circuit.

Figure 2.   Receiver

System operation

The exponentially decaying carrier is generated in the transmitter and encoded by a code previously selected by the user. The code is input through the keypad, which is a part of the front panel. As the carrier is generated, commands from the microprocessor are issued to the digitally controlled phase shifter to encode the carrier. Accordingly, for every bit of the code the carrier's phase is changed. The duration in time of every bit of the code is much smaller than the duration of the transmitted carrier. The encoded carrier is

40

amplified by a power amplifier and fed to a transmitting antenna. A reflected signal is received by the receiving antenna and three major operations are performed on it:

a. Envelope detection extracts the envelope of the returned carrier and generates a baseband signal characteristic of the target.

b. The returned signal is utilized to generate the complex reflection coefficient function. This function is then used as an input to a subcircuit in which an inversion is performed. As a result, electromagnetic profiles of the medium such as permittivity, conductivity, permeability, and susceptibility are generated.

c. The returned signal is digitized and digital signal processes are applied to it. The outputs from these three operations are features of the medium that is being identified.

4 Conclusions and Recommendations

Conclusions

Through examples presented in this report, it is demonstrated that the inverse problem is an ill-posed problem. In two formulations of this problem discussed in this report, there is not enough information available that may lead to an exact inversion procedure. Thus, approximate inversion procedures are sought. In case of electromagnetic propagation, which is the case investigated in this report, solutions of inverse problems are profiles such as permittivity, conductivity, and permeability. Such solutions have applications in target recognition. Specifically, in real-time automatic target recognition, the speed by which these profiles are generated is considered important. Furthermore, accuracies of these results have vital consequences on the recognition process. Deriving a solution for the inverse problem in dispersive scattering theory is generally difficult. In this report the pseudospectral Legendre method was used to find the dispersive properties of a homogeneous medium, i.e., the susceptibility kernel $G(t)$, by means of scattering methods. The method is based on representing the solution, i.e., $G(t)$, in terms of its value at Legendre-Gauss-Lobatto nodes. As a result, the inverse problem was reduced to a problem of solving a system of algebraic equations. In another inverse problem where the unknown was the potential function, the formulation of the inverse problem was based on the Gel'fand-Levitan integral equation. However, it was decided that explicit solutions of the Gel'fand-Levitan integral equation were seldom easy to obtain. Through the formulation procedure, the solution for the potential function produces several valuable and useful equalities. Accordingly, the application of the pseudospectral Legendre method to these equalities was considered. The method was based on representing a kernel $K(z,y)$ in terms of its value at Legendre-Gauss-Lobatto nodes. The approximate solution of the inverse example was generated under conditions produced through the differentiation of the Gel'fand-Levitan integral equation. As a result, the inverse problem was reduced to a problem of solving a system of algebraic equations. In another formulated inverse problem the solution was to find the scattering potential from given scattering information. In this formulation two Gel'fand-Levitan-Marchenko integral equations were associated with the Zakharov-Shabat partial differential equations. Two kernels, $A_1(x,y)$ and

$A_2(x,y)$, together with $R(x)$, which is the Fourier transform of the complex reflection coefficient, were used to express these integral equations. Again, the pseudospectral Legendre method was used to solve this inverse scattering problem. The method uses $R(x)$ as an input and generates values of the unknown potential function at the Legendre-Gauss-Lobatto nodes. Thus the problem was reduced to one of solving a system of algebraic equations. The rapid rate of convergence of the pseudospectral Legendre approximations (Gottlieb, Hussaini, and Orszag 1984) and the δ function property given in Chapter 2, "Application of the Legendre-Gauss-Lobatto collocation method to Zakharov-Shabat equations," make the approach used to solve the three inverse problems given in this report very attractive. The method is efficient and yields accurate results. Numerical examples furnished in this report support these claims.

Recommendations

The new Legendre-Gauss-Lobatto inversion scheme formulated in this report was applied to solve three inverse problems. The results from these three solutions were compared to corresponding solutions from other methods. The new scheme produced accurate results. However, the unknowns in these problems were one-dimensional. The following is a list of recommendations regarding the future of this new scheme:

a. Carry out a study of the effect of noise on the performance of the new scheme.

b. Perform detailed parametric study.

c. Apply the new scheme to the two-dimensional case and examine its performance.

d. Develop the high-resolution radar.

e. Utilize the high-resolution radar along with the new developed scheme in a target recognition procedure for evaluation purposes.

References

Askey, R. (1972). "Mean convergence of orthogonal series and Lagrange interpolation," *Acta Math. Acad. Sci. Hung.* 23, 71-85.

Beezley, R. S., and Krueger, R. J. (1985). "An electromagnetic inverse problem for dispersive media," *J. Math. Phys.* 26, 317-325.

Bleistein, N., and Cohen, J. K. (1977). "Nonuniqueness in the inverse source problem in acoustics and electromagnetics," *J. Math. Phys.* 18, 194-201.

Canuto, C., Hussaini, M. Y., Quarteroni, A., and Zang, T. A. (1988). *Spectral method in fluid dynamics*. Springer-Verlag, New York.

Chew, W. C., and Wang, Y. M. (1990). "Reconstruction of two-dimensional permittivity distribution using the distorted Born iterative method," *IEEE Trans. on Med. Img.* 9, 218-225.

Cui, T. J., and Liang, C. H. (1993). "Reconstruction of the permittivity profile of an inhomogeneous medium using an equivalent network method," *IEEE Trans. on Ant. and Prop.* 41, 1719-1726.

_____. (1994a). "Nonlinear differential equation for the reflection coefficient of a pure conducting medium and its novel inverse scattering solution," *IEEE Trans. on Geosci. and Remote Sens.* 32, 709-712.

_____. (1994b). "Nonlinear differential equation for the reflection coefficient of an inhomogeneous lossy medium and its inverse scattering solution," *IEEE Trans. on Ant. and Prop.* 42, 709-712.

_____. (1995). "Novel applications of an approximate profile inversion for one-dimensional medium," *IEEE Trans. on Ant. and Prop.* 43, 308-312.

Davis, P. J. (1963). *Interpolation and approximation.* Blaisdell, New York.

Devaney, A. J. (1983). "A computer simulation study of diffraction tomography," *IEEE Trans. on Biomed. Eng.* BME-30, 377-386.

Eaves, J. L., and Reedy, E. K., eds. (1987). *Principles of modern radar.* Reinhold, New York.

Frangos, P. V., and Frantzeskakis, D. J. (1993). "Pulse propagation in a non-linear optical fiber of parabolic index profile by direct numerical solution of the Gel'fand-Levitan integral equation," *IEE Proc.-J* 140, 141-149.

Frangos, P. V., and Jaggard, D. L. (1991). "A numerical solution to the Zakharov-Shabat inverse scattering problem," *IEEE Trans. on Ant. and Prop.* 39, 74-79.

_____. (1992). "Analytical and numerical solution to the two-potential Zakharov-Shabat inverse scattering problem," *IEEE Trans. on Ant. and Prop.* 40, 399-404.

Ge, D. B. (1987). "Reconstruction of conductivity profiles from pulse response," *IEEE Trans. on Ant. and Prop.* AP-35, 1185-1187.

Gel'fand, I. M., and Levitan, B. M. (1955). "On the determination of a differential equation by its spectral function," *Am. Math. Soc. Transl.* 1, 253-304.

Gottlieb, D., Hussaini, M. Y., and Orszag, S. A. (1984). "Theory and application of spectral method." *Spectral Method for Partial Differential Equation.* R. Vought, D. Gottlieb, and M. Y. Hussaini, ed., Society for Industrial and Applied Mathematics, Philadelphia.

Jackson, J. D. (1975). *Classical electrodynamics.* 2d ed., John Wiley, New York.

Jordan, A. K., and Kritikos, H. N. (1973). "An application of one-dimensional inverse-scattering theory for inhomogeneous regions," *IEEE Trans. on Ant. and Prop.*, 909-911.

Jordan, A. K., and Ladouceur, H. D. (1987). "Renormalization of an inverse scattering theory for discontinuous profiles," *Phys. Rev.* A, 4245-4253.

Kay, I. (1955). "The inverse scattering problem," Research Report EM-74-NY, Institute of Mathematical Sciences, Electromagnetic Research, New York University, New York.

_____. (1960). "The inverse scattering problem when the reflection coefficient is a rational function," *Communication on Pure and Applied Mathematics* XIII, 371-393.

Kincanon, E. (1993). "Approximate solution to the Gel'Fand-Levitan equation," *App. Math. and Comp.* 53, 121-128.

Kreider, K. L. (1989). "Time dependent inverse scattering from gradient-type interface using an exact solution," *J. Math. Phys.* 30, 53-58.

Kristensson, G., and Krueger, R. J. (1986). "Direct and inverse scattering in the time domain for a dissipative wave equation," *J. Math. Phys.* 27, 1667-1682.

Kritikos, H. N., Jaggard, D. L., and Ge, D. B. (1982). "Numeric reconstruction of smooth dielectric profiles," *Proceedings of the IEEE* 70, 295-297.

Krueger, R. J. (1978). "An inverse problem for an absorbing medium with multiple discontinuities," *Quart. of App. Math.*, 235-253.

Ladouceur, H. D., and Jordan, A. K. (1985). "Renormalization of an inverse scattering theory for inhomogeneous dielectrics," *J. Opt. Soc. Am* A 2, 1916-1921.

Lamb, G. L. (1980). *Elements of soliton theory*. Wiley, New York.

Marchenko, V. A. (1955). "Reconstruction of the potential energy from the phase of scattered waves," *Dokl. Akad. Nauk* SSR 104, 695-698.

Moghaddam, M. (1991). "Forward and inverse scattering problem in the time domain," Ph.D. diss., University of Illinois, Urbana.

Moses, H. E., and deRidder, C. M. (1963). "Properties of dielectrics from reflection coefficients in one dimension," Technical Report No. 322, Lincoln Laboratory, Massachusetts Institute of Technology, Boston.

Newton, R. G. (1981). "Inverse scattering II.," *J. Math Phys.* 21(7), 1698-1715.

Razzaghi, M., and Ahmad, F. (1995). "A collocation-type method for the solution of inverse problems in dispersive scattering theory," *Microwave and Opt. Tech. Letters* 9, 14-17.

Reilly, M. H., and Jordan, A. K. (1981). "The applicability of an inverse method for reconstruction of electron-density profiles," *IEEE Trans. Antennas Propagat.* Ap-29, 245-252.

Santosa, F., Pao, Yih-Hsing, Symes, W. W., and Holland, C., ed. (1984). "Inverse problems of acoustic and elastic waves," Society for Industrial and Applied Mathematics, Philadelphia.

Song, G. H., and Shin, S. Y. (1985). "Design of corrugated waveguide filters by the Gel'fand-Levitan-Marchenko inverse-scattering method," *J. Optic. Soc. Am. A* 2, 1905-1915.

Tijhuis, A. G., and Van Der Worm, C. (1984). "Iterative approach to the frequency-domain solution of the inverse-scattering problem for an inhomogeneous lossless dielectric slab," *IEEE Trans. on Ant. and Prop.* 32, 711-716.

Ulaby, F. T., Moore, R. K., and Fung, A. K. (1981). "Microwave remote sensing," *Fundamentals and radiometry*, Vol. I, Artech House, MA.

Weston, V. H. (1972). "On the inverse problem for a hyperbolic dispersive partial equation," *J. Math Phys.* 13, 1952-1956.

Wolfgang-Martin, B., Jordan, A. K., and Kay, I. W. (1981). "Introduction to the special issue on inverse methods in electromagnetics," *IEEE Trans. On Ant. And Prop.* AP-29, 185-189.

Appendix A
Notation

B Bandwidth of a transmitted signal

c Speed of light

$D(x,t)$ Displacement field

$E^-(x,t), E^+(x,t)$ Left- and right-moving electromagnetic waves, respectively

$E(x,t)$ Electromagnetic field

$E_{tt}(x,t)$ Second partial derivative of electrical field intensity with respect to the variable of t

$E_{xx}(x,t)$ Second partial derivative of electrical field intensity with respect to the variable of x

$E_{zz}(z,t)$ Second partial derivative of electrical field intensity with respect to the variable of z

G Susceptibility kernel

j Constant, $\sqrt{-1}$; index

L Depth of medium

$L_N(t)$ Legendre polynomial of order N

$L_N'(t)$ First derivative of $L_N(t)$

$r(x,t)$ Impulse response of the inhomogeneous medium

$r(\kappa)$ Complex reflection coefficient

R Impulse response

A1

S Scattering matrix of transmission line junction

t Time; variable in the Legendre polynomial

T Temporal length of the impulse response; duration of an uncoded transmitted radar signal

$v(z)$ Potential function

x Depth in the dielectric inhomogeneous medium

$Z(x)$ and $Z(x+dx)$ Wave impedances at the points x and $x + dx$, respectively

z Depth in the medium

δ_r Range resolution of an uncoded transmitted radar signal

ε_0 Permittivity of free space

$\varepsilon(z)$ Dielectric permittivity

κ Wave number

μ_0 Permeability

$\rho(\kappa,x)$ Frequency domain reflection coefficient of the medium

τ Duration of each pulse of an uncoded transmitted radar signal

ω Radial frequency

A2

REPORT DOCUMENTATION PAGE

Public reporting burden for this collection of information is estimated to average 1 hour per response, including the time for reviewing instructions, searching existing data sources, gathering and maintaining the data needed, and completing and reviewing the collection of information. Send comments regarding this burden estimate or any other aspect of this collection of information, including suggestions for reducing this burden, to Washington Headquarters Services, Directorate for Information Operations and Reports, 1215 Jefferson Davis Highway, Suite 1204, Arlington, VA 22202-4302, and to the Office of Management and Budget, Paperwork Reduction Project (0704-0188), Washington, DC 20503.

1. AGENCY USE ONLY (Leave blank)	2. REPORT DATE May 1996	3. REPORT TYPE AND DATES COVERED Final report

4. TITLE AND SUBTITLE
Approximation of Electromagnetic Profiles

5. FUNDING NUMBERS

6. AUTHOR(S)
Falih H. Ahmad

7. PERFORMING ORGANIZATION NAME(S) AND ADDRESS(ES)
U.S. Army Engineer Waterways Experiment Station
3909 Halls Ferry Road, Vicksburg, MS 39180-6199

8. PERFORMING ORGANIZATION REPORT NUMBER
Technical Report ITL-96-2

9. SPONSORING/MONITORING AGENCY NAME(S) AND ADDRESS(ES)
Discretionary Research Program
U.S. Army Engineer Waterways Experiment Station
3909 Halls Ferry Road, Vicksburg, MS 39180-6199

10. SPONSORING/MONITORING AGENCY REPORT NUMBER

11. SUPPLEMENTARY NOTES
Available from National Technical Information Service, 5285 Port Royal Road, Springfield, VA 22161.

12a. DISTRIBUTION/AVAILABILITY STATEMENT
Approved for public release; distribution is unlimited.

12b. DISTRIBUTION CODE

13. ABSTRACT (Maximum 200 words)

A numerical scheme for profile inversion is proposed in this report. The numerical scheme utilizes interpolating polynomials as a tool for near real-time inversion. In addition, linear transformations are used in the scheme. In general, the scheme uses the impulse response or the complex reflection coefficient from a tested medium as an input. It converts inverse problems formulated in the form of integral, partial differential, or differential equations to sets of algebraic equations. Solutions of these equations are approximations of the electromagnetic profiles of the tested media. The scheme is applied to solve different examples, and results from these solutions are compared with those produced through the applications of other methods and presented in published references or with results generated analytically. Accuracy and efficiency of the proposed scheme are addressed through such comparisons.

14. SUBJECT TERMS
Inverse problem
Material characterization
Profile inversion

15. NUMBER OF PAGES
58

16. PRICE CODE

17. SECURITY CLASSIFICATION OF REPORT UNCLASSIFIED	18. SECURITY CLASSIFICATION OF THIS PAGE UNCLASSIFIED	19. SECURITY CLASSIFICATION OF ABSTRACT	20. LIMITATION OF ABSTRACT